Journal of Catalysis 269 (2010) 15–25

Contents lists available at ScienceDirect

Journal of Catalysis

journal homepage: www.elsevier.com/locate/jcat

Catalytic properties of dendron–OMS hybrids

Qingqing Wang, Victor Varela Guerrero, Anirban Ghosh, Seunguk Yeu, Jonathan D. Lunn, Daniel F. Shantz *

Artie McFerrin Department of Chemical Engineering, Texas A&M University, College Station, TX 77843-3122, United States

ARTICLE INFO

Article history:
Received 2 September 2009
Revised 8 October 2009
Accepted 8 October 2009
Available online 14 November 2009

Keywords:
Ordered mesoporous silica
Organocatalysts
Dendrons
Aldol reactions

ABSTRACT

The synthesis and catalytic testing of several dendron–ordered mesoporous silica hybrids are reported. These materials are active in both the nitroaldol (Henry) reaction and the transesterification of glyceryl tributyrate to afford methyl esters. In both reactions it is observed that dendrons terminated with primary amines are more catalytically active than samples containing dendrons terminated with secondary amines. On a mmol nitrogen per gram of silica basis, the first generation dendrons are the most active for both chemistries, and the SBA-15 samples display a higher activity than the MCM-41 samples. The pore-size effect observed is consistent with significant diffusion resistance in the MCM-41 samples. The activity trend observed in the SBA-15 materials is consistent with decreased cooperative effects between the amines and surface silanols as the dendrons become larger. Clear trends are observed indicating that higher generation dendrons are more selective to alcohol formation in the Henry reaction. The dendron catalysts are much more active and stable than simple amines attached to silica in the transesterification of triglycerides. Preliminary results shown indicate that these materials can also catalyze more demanding chemistries, an example of which is the Aldol condensation of 5-(hydroxymethyl)furfural and acetone. The results shown indicate that dendron–OMS hybrids can serve as effective solid base catalysts for a diverse range of chemistries.

1. Introduction

Ordered mesoporous silicas (OMS) have attracted considerable interest in the last 15 years as potential adsorbents, catalysts/catalyst supports, sensors, etc. [1–8]. These materials possess several highly desirable properties: pore topologies that possess long-range structural ordering, uniform pore sizes in the 2–10 nm range, and high surface areas. While the pore structure often possesses long-range ordering the oxide phase is in fact amorphous. Another aspect of considerable interest in the current work is that the silanol groups present can be readily functionalized using well-known silane chemistry [3]. Thus these OMS phases represent a model substrate for fabricating well-defined organic–inorganic hybrid materials.

Numerous laboratories have reported on the synthesis of organic-functionalized OMS materials. Early works investigated materials containing simple chemical groups (e.g. amines, vinyl groups) and the properties of the resulting material [9–12]. Many works have compared the properties of OMS phases functionalized via post-synthetic grafting versus those made via co-condensation wherein the organic group is incorporated directly during synthesis. A fairly recent review by Hoffman et al. [2] has summarized many aspects of functionalized OMS materials. An early paper from the Stein Lab is also particularly noteworthy in this area [10]. More recently periodic mesoporous organosilicas (PMOs) have been developed, which represent composite materials with extremely high organic loadings.

Numerous laboratories have reported the synthesis and catalytic testing of OMS materials with organic groups attached. This literature has expanded enormously in recent years, and several reviews are available for the interested reader [1,4,13]. Given the scope of the current work, the area of amine–OMS materials will be briefly summarized. Many laboratories, including those of Brunel, Lin, Katz, Shimizu, Yoshitake, and Corma, have investigated the activity of amines on OMS phases for a variety of reactions including Aldol chemistry and Michael additions. [14–27]. The second body of work has focused on proline-derivatized and alkaloid-derivatized surfaces with the aim of making solid base catalysts for the production of chiral molecules [27,28]. A few laboratories, most notably the laboratories of Davis and Lin, have also investigated the synthesis of OMS materials containing multiple functional groups and their catalytic efficacy [20,21,29–32].

The fabrication of OMS-hybrid materials with high densities of organic functional groups is difficult in the sense that the distribution of catalytically active sites often becomes heterogeneous. Work by Jones' lab [33–35] and Katz's lab [14,15,36] has shown that surface patterning and molecular imprinting techniques to achieve higher densities of homogeneous organic functional groups can circumvent this issue. Another possible approach to

* Corresponding author. Fax: +1 979 845 6446.
E-mail address: Shantz@chemail.tamu.edu (D.F. Shantz).

0021-9517/$ - see front matter © 2009 Elsevier Inc. All rights reserved.
doi:10.1016/j.jcat.2009.10.009

obtain high organic group densities is the use of surface-tethered dendrimers. Linden's and Jones' laboratories have reported ring-opening polymerization of aziridine groups to generate hyperbranched polymers, although their catalytic properties are yet to be reported [37–40]. Recently our group has reported the immobilization of melamine-based dendrimers on the surfaces of amine-functionalized SBA-15 materials [41–43]. At approximately the same time, collaborative work between the Alper and Sayari laboratories reported similar investigations of PAMAM-based dendrons in large pore MCM-41 materials [44,45]. The current investigation, building off our previous reports, describes the catalytic testing of these materials in the Henry (nitroaldol) reaction, the synthesis of methyl esters from triglycerides, and the cross aldol reaction between acetone and 5-hydroxymethylfurfural.

2. Materials and methods

2.1. General

Sodium silicate (PQ Brand N, SiO_2 28.7%, SiO_2/Na_2O = 3.22), cetyltrimethylammonium bromide (CTAB, Fisher Chemical, high purity grade), H_2SO_4 (Sigma–Aldrich, 95–98% ACS reagent), sodium hydroxide (NaOH, Mallinckrodt Chemicals, pellet), tetraethoxysilane (TEOS, ⩾99%, Fluka), Pluronic P123 ($EO_{20}PO_{70}EO_{20}$, MW = 5800, BASF), and HCl (Sigma–Aldrich, reagent grade, 37%) were used in the OMS synthesis as received. 3-(Aminopropyl)triethoxysilane (APTES, 99%, Sigma–Aldrich), piperazine (Fluka, ⩾98%), diisopropylethylamine (DIPEA, 99%, Alfa Aesar), 4-(aminomethyl)piperidine (AMP, ⩾98%, TCI America), and cyanuric chloride (CC, 99%, ACROS) were used in the dendrimer synthesis as received. Tetrahydrofuran (THF, Sigma–Aldrich, ⩾99%) and toluene (Sigma–Aldrich, ⩾99.5%) were dried using standard methods using an MBraun solvent purification system. Methanol and dichloromethane (DCM) (ACS solvent grade) were purchased from EMD and used as received. Nitromethane (Acros, reagent ACS) and nitrobenzaldehyde (Fluka, ⩾99%, HPLC) were used as received for the Henry reaction. Glyceryl tributyrate (99%) was obtained from Sigma–Aldrich and was used as received in the transesterification reaction. All NMR analyses were performed in deuterated chloroform (Cambridge Isotope, 99.8% D, 1% V/V TMS).

2.2. Synthesis of MCM-41 and SBA-15

MCM-41 was synthesized using the reported procedure of Edler and White [46,47], and the SBA-15 samples were synthesized using the method reported by Zhao et al. [48]. As an example for the synthesis of MCM-41, 7.9 g of sodium silicate solution was mixed with 45.4 mL deionized water. NaOH (0.27 g) was added to the solution followed by the addition of 7.8 mL of 1 M H_2SO_4. CTAB (7.29 g) was dissolved in the solution and stirred for 15 min at room temperature. The mixture was then placed in an oven at 100 °C for 24 h under static conditions. After 24 h the sample was removed from the oven, allowed to cool sufficiently so that it could be easily handled, and titrated to a pH of approximately 10 using 1 M H_2SO_4. The sample was then placed back in the oven at 100 °C. The titration step was performed two additional times in regular 24-h intervals. The total heating period was 96 h. For the SBA-15 synthesis, 4.0 g of Pluronic P123 was dissolved in 60 mL of 4 M HCl and 85 mL of deionized water by stirring for 5 h at room temperature. Then, 8.5 g of TEOS was added to that solution and stirred for 24 h at 35 °C. The mixture was then aged at 80 °C for 24 h without stirring. After completion of the reaction, the solid products were filtered, washed with deionized water, and air-dried overnight. The solid products were calcined to remove CTAB or Pluronic. The calcination procedure was as follows: the air-dried samples were heated from room temperature to 100 °C at a rate of 1 °C/min; held at 100 °C for 2 h; increased from 100 to 500 °C at a rate of 1 °C/min; and then held at 500 °C for 8 h.

2.3. Synthesis of MCM-41/SBA-15–dendron hybrids

The synthesis method for generating the functionalized OMS materials is shown in Scheme 1. The amine-functionalized MCM-41 and SBA-15 samples were prepared using post-synthetic grafting. Unless noted otherwise the target loading of organic is 0.2 mmequiv./g SiO_2. One gram of calcined MCM-41 or SBA-15 was placed in a round-bottomed flask, and dried at 100 °C under vacuum for 1 h. Then, 100 mL of anhydrous toluene was added into the flask under nitrogen. An aliquot of APTES 46 μL (0.2 mmol) was added to the solution under nitrogen. This mixture was stirred overnight in a closed flask at room temperature. The product was collected by filtration, washed sequentially with 50 mL of toluene, 50 mL of methanol, and 500 mL of deionized water, and air-dried. The synthesis of the dendron–SBA-15/MCM-41 composites was performed as reported previously by our laboratory [41,42]. As an example for the case of the dendrons containing 4-(aminomethyl)piperidine as the linkers (i.e. AMP dendrons), a 0.3 M cyanuric chloride (CC) solution was prepared by adding 1.25 g of CC and 2.5 mL of diisopropylethylamine (DIPEA) (8 mmol) to 25 mL of THF. A 0.4 M 4-(aminomethyl)piperidine (AMP) solution was

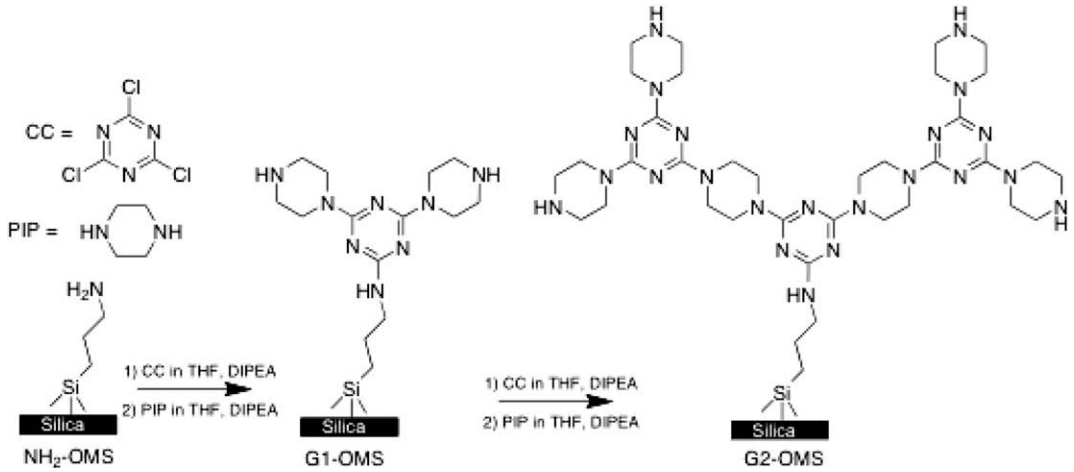

Scheme 1. Dendron synthesis from OMS surface illustrated with PIP.

prepared by adding 1.25 g of AMP to 25 mL of THF. One gram of amine-functionalized MCM-41 or SBA-15 was placed in a 30 mL vial, and 25 mL of the prepared CC solution was added. The vial was shaken for 24 h at room temperature. The solution was filtered, and rinsed with 50 mL portions of methanol, dichloromethane, and THF sequentially. The silica was transferred back to a clean vial, and 25 mL of the linker molecule solution (AMP or PIP) was added, and the vial was again shaken for 24 h. The material was filtered and rinsed as described above. This process was repeated to increase the dendron generation. Note that in all the results shown for a series of samples of different dendron generation, they are all derived from the same parent sample. For clarity, samples with dendrons made using 4-(aminomethyl)piperidine as the diamine linker are denoted as G**x** AMP dendrons, and samples with dendrons made using piperazine as the diamines linker are denoted as G**x** PIP dendrons where **x** is the dendron generation.

2.4. Analytical

Powder X-ray diffraction (PXRD) measurements were performed using a Bruker-AXS D8 powder diffractometer with Cu Kα radiation over a range of 0.5–10° 2θ. Infrared spectroscopy was recorded using a Nexus 670 FT-IR spectrometer from Thermo Nicolet. Thermal gravimetric analyses (TGA) were performed using a TG 209C Iris instrument from Netzsch over a temperature range of 25–500 °C using oxygen and nitrogen as carrier gases and a temperature ramping rate of 1 °C/min. Nitrogen-adsorption experiments were performed on a Micromeritics ASAP 2010 micropore system using approximately 0.06 g of sample. The samples were degassed under vacuum at room temperature for 2 h, then at 100 °C for 24 h before analysis. The mesopore volumes and surface areas were determined using the α_s-method [49,50]. The surface areas were determined from the slope of the linear portion of the α_s-plot over the range $0 \leqslant \alpha_s \leqslant 0.6$, and the mesopore volumes were determined from the *y*-intercept of the tangent line taken over the range $1.5 \leqslant \alpha_s \leqslant 2.0$. The mesopore size distributions were calculated from the adsorption branch of the isotherms using the Barret–Joyner–Halenda (BJH) method with a modified equation for the statistical film thickness. Solid-state NMR experiments were performed at 9.4 T on a Bruker Avance. $^{13}C\{^1H\}$ CP-MAS were performed at 100.61 MHz using a 4 mm probe with ZrO_2 rotors, a spinning rate of 9 kHz, a contact time of 2 ms, a ^1H 90° pulse length of 2.5 μs, and a recycle delay of 5 s. Chemical shifts were referenced to tetramethylsilane. Elemental analysis (Si, C, H, and N analysis) was performed by the Galbraith laboratories.

2.5. Catalytic testing

Scheme 2 shows the three reactions investigated in this work. The nitroaldol reaction (Henry reaction) was performed as follows. One hundred milligrams of the catalyst was placed in a 10 mL Schlenk tube with a small stir bar, and heated in an oven at 100 °C overnight. Upon cooling, 0.38 g of nitrobenzaldehyde (2.5 mmol) and 1.35 mL of nitromethane (25 mmol) were introduced into the tube. The mixture in the tube was kept at 40 °C under stirring. At different time intervals 100 μL of the solution was transferred into a small glass tube, 1 mL of deuterated chloroform was added to the tube, and then the solid was removed from the solution using a centrifuge. The liquid was analyzed by ^1H NMR. The conversion was calculated from the relative intensity of the nitrobenzaldehyde peak (δ 9.9–10.1 ppm, 1H) and 1-(4-nitrophenyl)-2-nitroethanol peak (δ 5.58–5.64 ppm, 1H).

The transesterification reaction of glyceryl tributyrate with methanol was performed as follows: to a 50 mL flask equipped with a stir bar and a condenser, glyceryl tributyrate (GTB) and methanol were added in a 1:10 weight ratio (0.5 g GTB:5 g MeOH).

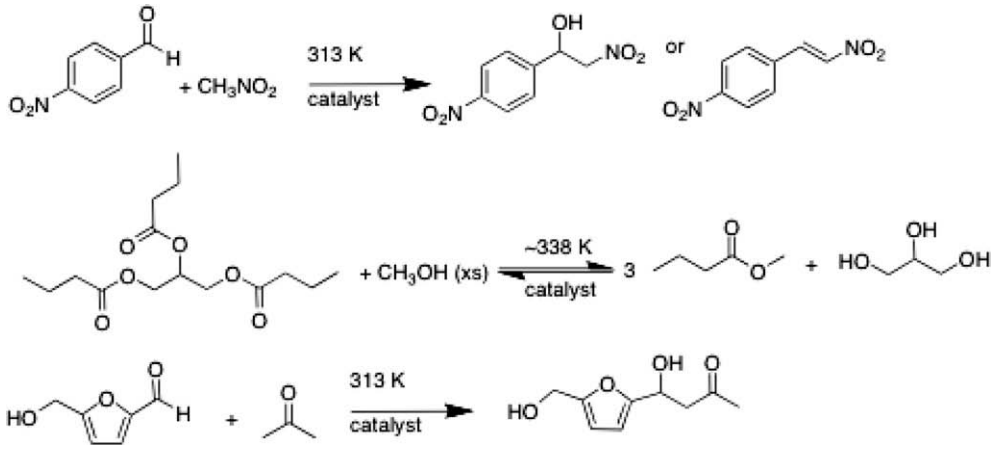

Scheme 2. Reactions investigated in the current work. From top to bottom: Henry reaction, methyl ester synthesis from triglycerides, and Aldol condensation of 5-(hydroxymethyl)furfural (HMF) with acetone.

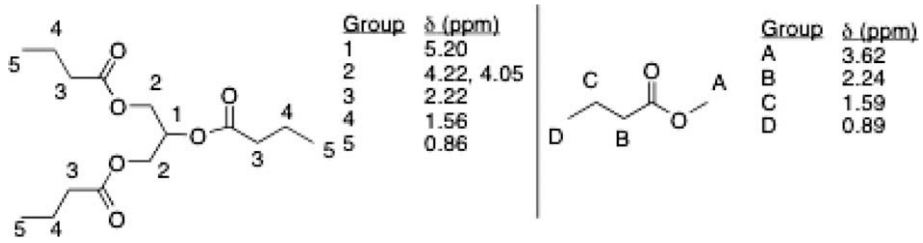

Scheme 3. Molecular structures of GTB and the methyl ester product, and chemical shifts of the different protons as determined by ^1H NMR.

The catalyst (0.175 g) was then added. All reactions were run at reflux (~65 °C) for 6 h. At the end of the reaction period the flask was placed in an ice bath to quench the reaction, and the solids were separated by centrifugation and the liquid phase was isolated. For kinetics measurements of conversion versus time, aliquots were taken out at the time intervals noted. The conversion of the glyceryl tributyrate to methyl ester was determined from the relative intensities of the methyl ester protons (δ = 3.6 ppm, group A in Scheme 3) and methylene protons adjacent to the ester group (δ = 2.2 ppm, group 3 and group B in Scheme 3) as has been done previously [51]. For the recycle studies, the recovered catalyst was rinsed with 20 mL of methanol three times, dried overnight at 40 °C, and the testing was repeated.

The Aldol condensation of 5-hydroxymethylfurfural (HMF) with acetone was also investigated. One hundred milligrams of the catalyst was placed in a 10 mL Schlenk tube with a small stir bar, and heated in an oven at 100 °C overnight. Upon cooling, 0.32 g of HMF (2.5 mmol) and 1.83 mL of acetone (25 mmol) were introduced into the tube. The mixture in the tube was kept at 40 °C under stirring. At different time intervals 100 μL of the solution was transferred into a small glass tube, 1 mL of deuterated chloroform was added to the tube, and then the solid was removed from the solution using a centrifuge. The liquid was analyzed by ^{1}H NMR. The conversion was calculated from the relative intensity of the furfural (δ 9.6 ppm, 1H) and the product peak (δ 4.5–4.6 ppm, 2H).

The catalytic data presented for the Henry reaction and transesterification reaction are presented as both absolute conversion of reactant and amount of substrate consumed (or product formed) per mmol of nitrogen per gram of silica. The latter is an attempt to normalize the reactivity data to an effective mmol of amine basis, as different samples have different amine contents.

3. Results and discussion

3.1. Hybrid characterization

Fig. 1 shows the powder XRD patterns of representative parent MCM-41 and SBA-15 materials used in all subsequent work. As can

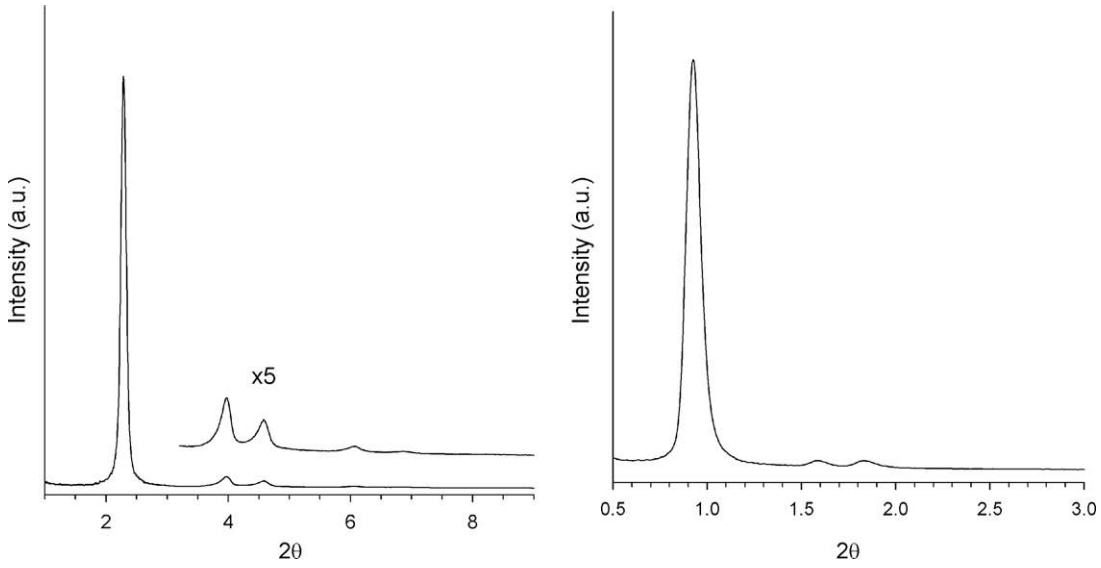

Fig. 1. PXRD patterns of (left) MCM-41 and (right) SBA-15.

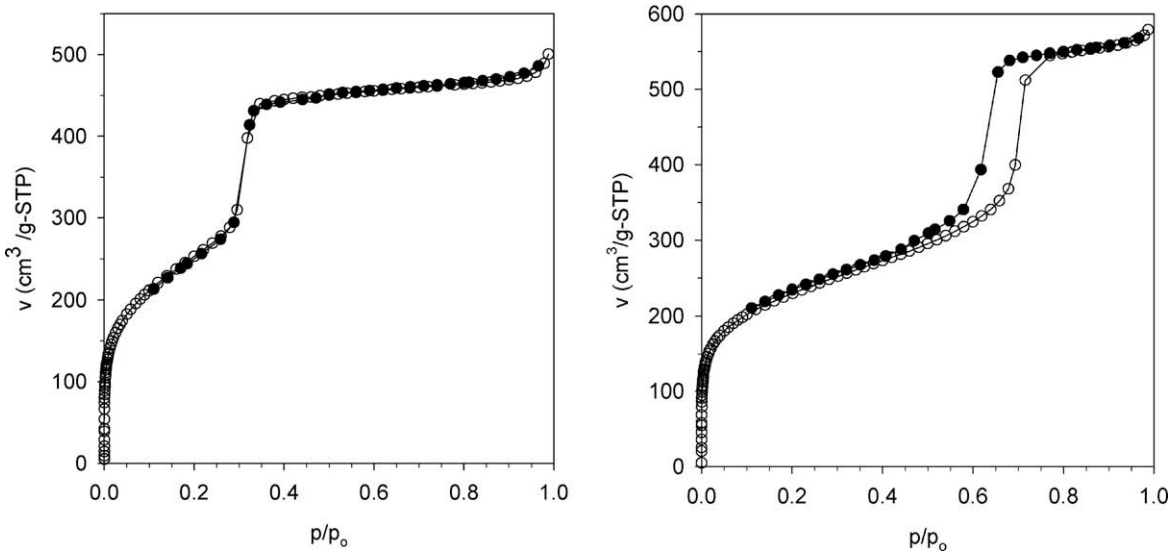

Fig. 2. Nitrogen adsorption isotherms of (left) MCM-41 and (right) SBA-15. Adsorption branches are represented by open circles; desorption branches by solid circles.

Table 1
Summary of adsorption data of the OMS-hybrid materials.

Sample	$S(\alpha_s)$ (m^2/g)	$v_{meso}(\alpha_s)$ (cm^3/g)	d_{BJH} (nm)
MCM-41	906	0.68	3.5
NH_2-MCM-41	814	0.61	3.4
G1-AMP-MCM-41	597	0.40	3.0
G2-AMP-MCM-41	~0	~0	
G3-AMP-MCM-41	~0	~0	
G1-PIP-MCM-41	665	0.45	3.0
G2-PIP-MCM-41	408	0.22	3.0
G3-PIP-MCM-41	~0	~0	
SBA-15	766	0.78	7.8
NH_2-SBA-15	523	0.70	7.9
G1-AMP-SBA-15	401	0.56	7.9
G2-AMP-SBA-15	337	0.48	7.9
G3-AMP-SBA-15	320	0.43	7.5
G1-PIP-SBA-15	407	0.53	7.8
G2-PIP-SBA-15	339	0.43	7.5
G3-PIP-SBA-15	312	0.32	6.4

be observed the syntheses lead to highly ordered OMS materials. In the case of the MCM-41 samples four reflections are clearly observed and the fifth is weakly visible. For the SBA-15 materials there are three reflections. The PXRD patterns of all samples are included in the Supplementary material. Consistent with previous work the higher order reflections become weaker as the organic content of the hybrid material increases and no appreciable change in the peak positions is observed. The PXRD results show that the parent materials are well-defined MCM-41 and SBA-15 materials.

Nitrogen adsorption was used to quantify the change in porosity of all samples. The adsorption isotherms of the parent OMS materials are shown in Fig. 2 and data for all of the samples are summarized in Table 1. The isotherms shown in Fig. 2 are consistent with those reported in the previous work. The nominal pore sizes of the parent MCM-41 and SBA-15 are 3.5 and 7.8 nm, respectively. Several observations can be made from the data summarized in Table 1. First, in the case of the AMP-MCM-41 samples it

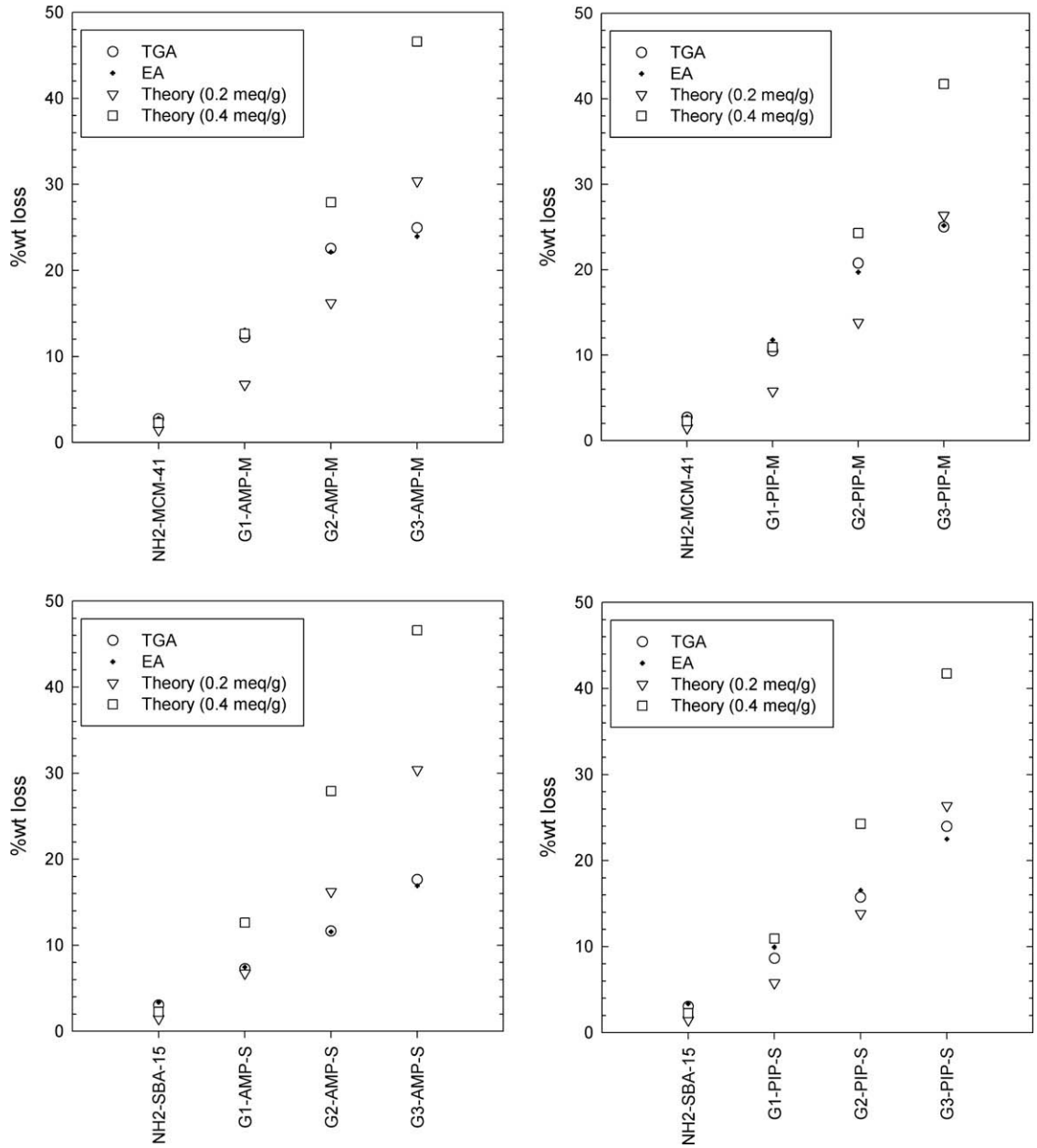

Fig. 3. Plots comparing elemental analysis and TGA results along with theoretical weight losses assuming 100% conversion at every step.

appears that for both dendrons investigated the resulting G2 and G3 hybrids are non-porous, at least based on nitrogen porosimetry. Given the relatively small (3.5 nm) pore size of the parent OMS this does not seem entirely unreasonable. The G1-PIP dendron should be modestly smaller as this sample appears to have both a slightly higher surface area and pore volume (~10% larger) than the AMP sample. Also note that while the G2-PIP sample has some porosity based on nitrogen adsorption, the G3 sample does not. The SBA-15 samples on the whole show similar trends to the materials reported previously by our laboratory at low amine loading. However, in contrast to our previous work with a nominal amine loading of 0.5 mmequiv./g, here we observe a systematic decrease in pore volume from amine-functionalized SBA-15 to G1 to G2 samples. The pore sizes, as manifested by the position and width of the capillary condensation hysteresis loop, do not change appreciably. The change in pore volumes from G2 to G3 is smaller than would be expected for both samples; this will be discussed in more detail below in the context of the TGA and EA data. One possible explanation for this is pore mouth blockage/preferential formation of dendrimers at the pore mouth due to preferential attachment of the silane at the pore mouth opening. At the most cautious level, the adsorption data clearly show that a significant portion of the organic content attached to the surface is in the mesopores given the pronounced decreases in the pore volume. The α_s-plots for all the samples are included in the Supplementary material.

The amount of organic content occluded in the materials was determined by elemental analysis and thermogravimetric analysis. These results are summarized in Fig. 3, along with calculations showing ideal weight loadings if every step proceeded at 100% efficiency. In general, the elemental analysis and TGA data are in very good agreement. However, the organic content of the amine–OMS samples is much higher (2.5–3-fold times larger) than would be predicted theoretically as are the G1 samples. NMR measurements do not show the presence of alkoxy groups. The TGA/EA results also indicate, consistent with the nitrogen adsorption data, that the reaction of converting the G2-MCM-41 materials to G3-MCM-41 materials is generally inefficient. The data shown in Fig. 3 are included in the Supplementary material. Fig. 4 shows the mmol of nitrogen per gram of silica for each of the samples as determined by elemental analysis. Several observations can be made from these data. The results shown here reinforce the conclusions from Fig. 3. These include that the chemistry is inefficient in converting G2 dendrons to G3 dendrons, particularly for the AMP diamine. It also shows that conversion of the aminosilica to G1 dendrons is less efficient on SBA-15 than on MCM-41. We have observed this previously, and one possible explanation consistent with our prior work is that some of the amines preferentially graft into the micropores of SBA-15 and thus are inaccessible for further functionalization. If the chemistry went perfectly (i.e. 100% conversion at every step) the ratio of nitrogen should be 8:22:50 (1:2.75:6.25); as can be seen this is not observed. The motivation for showing Fig. 4 is that all the catalytic data will be presented as mmol of substrate consumed (or product formed) per mmol of nitrogen per gram of silica. Also, for the catalytic data shown the activity is normalized per mmol of nitrogen and not per mmol of periphery amines. In other words, the authors did not attempt to ascertain which fraction of the nitrogen atoms participate in the reaction. While it is not expected that the nitrogen centers on the cyanuric

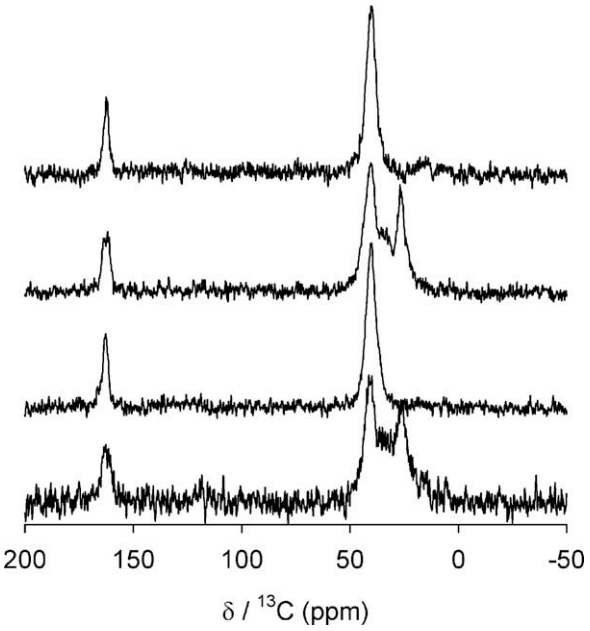

Fig. 5. $^{13}C\{^1H\}$ CP MAS NMR spectra of (from top to bottom): G3-PIP-MCM-41, G3-AMP-MCM-41, G3-PIP-SBA-15, and G3-AMP-SBA-15.

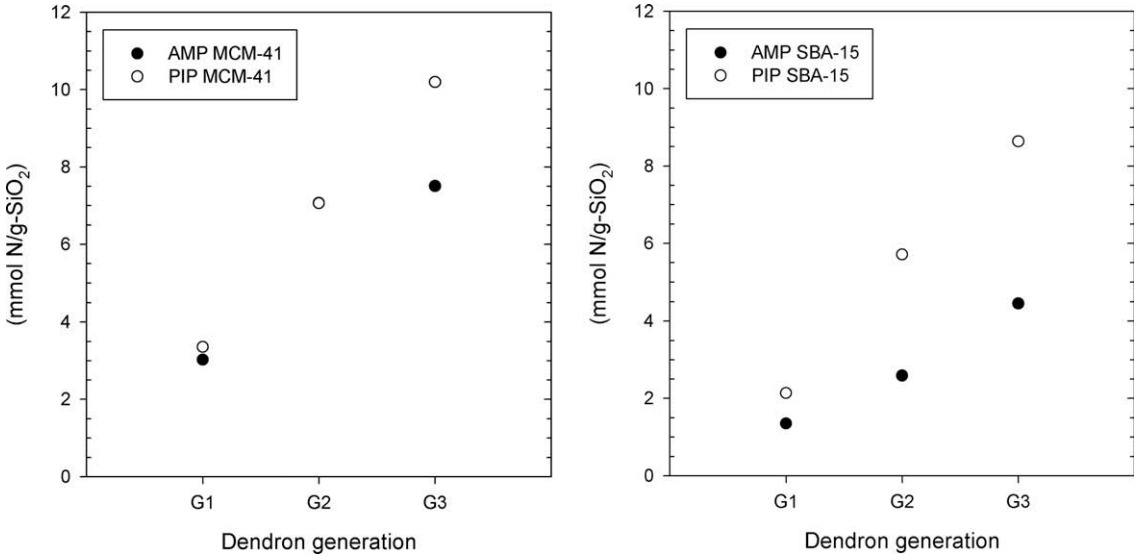

Fig. 4. Nitrogen loading for the different samples as determined by elemental analysis. Note that for the G2-MCM-41 samples the mmol N/g-SiO_2 are essentially identical (i.e. the data markers overlap).

chloride, for instance, participate in the reaction it is unclear if (whether) the interior aliphatic amines do. Thus, given the consistency between the TGA and elemental analysis results the authors thought it appropriate to normalize based on the total nitrogen content.

Evidence for organic group incorporation is obtained from $^{13}C\{^{1}H\}$ CP MAS NMR (Fig. 5). The signal at 163 ppm is attributed to the aromatic carbons. The two resonances at approximately 40 and 25 ppm for the AMP-dendron hybrid samples are due to the aliphatic carbons of the 4-(aminomethyl)piperidine group. For the PIP-dendron hybrid samples the signal at 163 ppm is also due to the aromatic carbons from CC groups. The other strong signal at approximately 40 ppm is from the aliphatic carbons on piperazine groups.

3.2. Catalytic testing, nitroaldol reaction

As several laboratories have investigated the nitroaldol reaction over amine–OMS materials we thought this was an appropriate test reaction to study the catalytic properties of our dendron–OMS materials. Fig. 6 shows the conversion versus time and mmol of aldehyde consumed per mmol nitrogen per gram silica for the MCM-41-dendron composites. All samples (on a percent conversion basis) appear to possess reasonable activity for this reaction. When the conversion is normalized to the mmol of nitrogen per gram of silica several trends emerge. First, it becomes clear for both samples that the G1 dendron hybrids are more active. Second, the AMP samples (on per mmol nitrogen basis) are also more active. Also noteworthy is that on a per site basis the G2 and G3 samples appear essentially identical. There are a few possible explanations for the decrease in activity of the higher generation dendrons. The first is that there are diffusion resistances present in the MCM-41 composites. The second is that the intrinsic activity of the sites decreases with increasing number densities of amines. The third, related to the second reason, is that as the dendron fragment gets larger there are less amine–silanol interactions. Based on the results mentioned below for the SBA-15 samples, we discount that

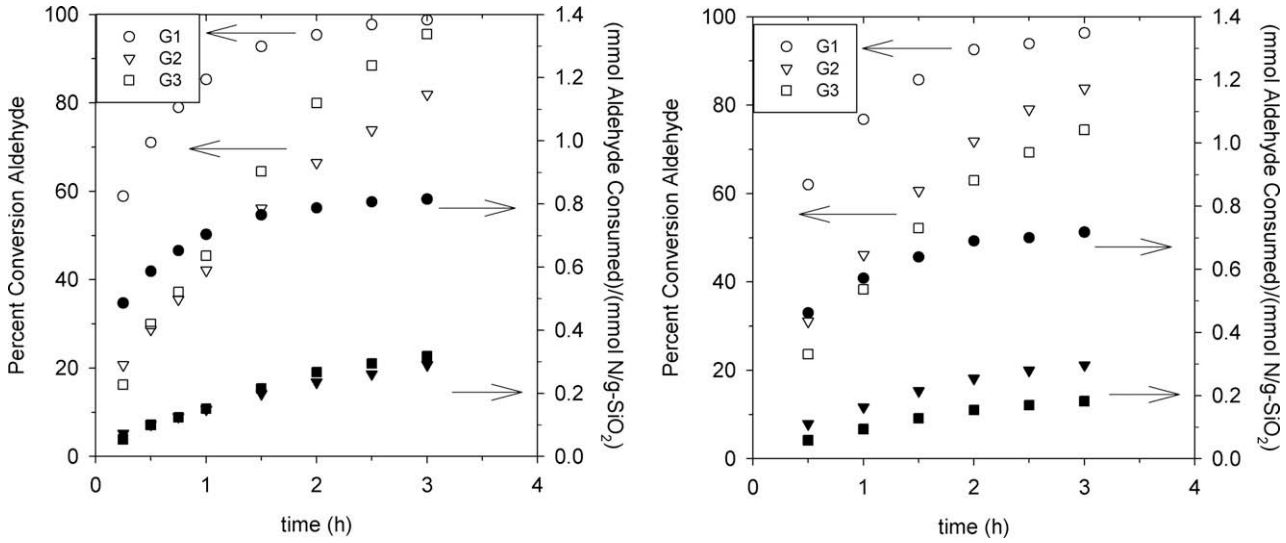

Fig. 6. Conversion of aldehyde (left axis) and mmol aldehyde consumed per mmol nitrogen per gram of silica (right axis) versus time for AMP (left) and PIP (right) dendrons supported on MCM-41 in the nitroaldol reaction. Dendron generation denoted, solid symbols correspond to right axis, open symbols to left axis.

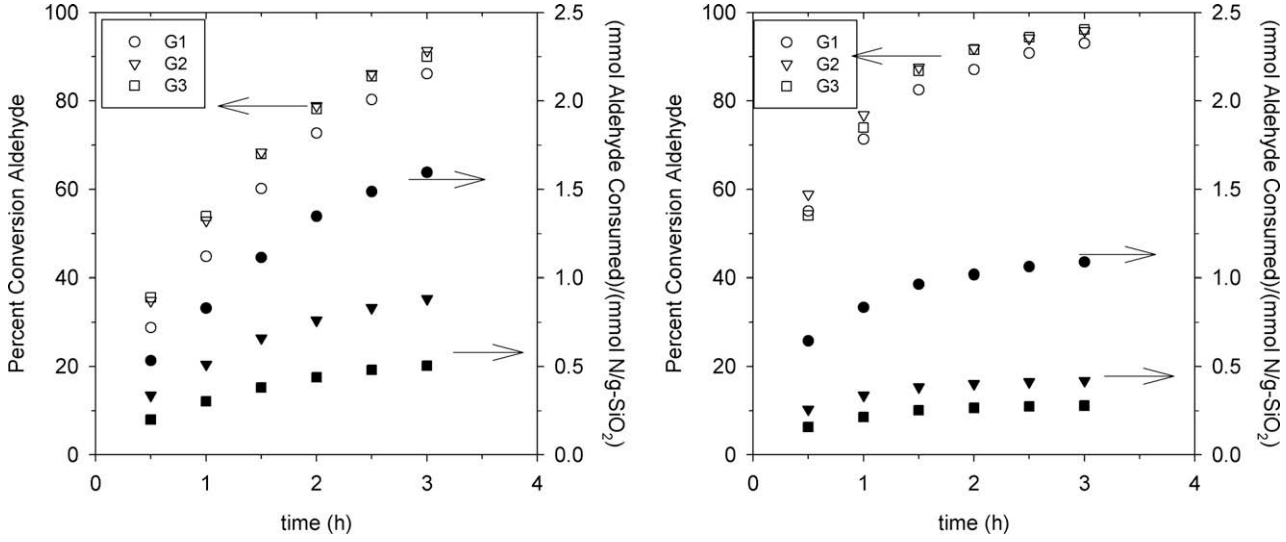

Fig. 7. Conversion of aldehyde (left axis) and mmol aldehyde consumed per mmol nitrogen per gram of silica (right axis) versus time for AMP (left) and PIP (right) dendrons supported on SBA-15 in the nitroaldol reaction. Dendron generation denoted, solid symbols correspond to right axis, open symbols to left axis.

the decreased activities observed can be solely attributed to diffusion effects.

Different generations of dendrimers, with AMP and PIP functional groups, on SBA-15 were also investigated (Fig. 7). Again, on a percent conversion basis all samples appear active and comparable. When normalized to the nitrogen loading, however, some clear differences can be observed. First, these materials are more active on a per site basis than the MCM-41 samples, and there are clear differences in activity between G2 and G3 samples. This point can likely be assigned to the absence (or decrease) of diffusion resistances. The AMP samples are again more active than the PIP samples, and again the G1 samples are much more active than the G2 and G3 samples. Taking the results in Figs. 6 and 7 together, a few observations can be made. First, it appears that upon going to larger pored silicas the intrinsic reactivity of the dendrimers goes down with increasing dendron generation. The authors ascribe this to decreased amine–silanol interactions. The SBA-15 G2/G3 samples show statistically significant differences in reactivity in contrast to the MCM-41 G2/G3 samples. This likely indicates that for the MCM-41 samples significant diffusion resistances are present. The increase in the G1-AMP-SBA-15 reactivity as compared to the G1-AMP-MCM-41 sample also supports the presence of diffusion resistances in the MCM-41 composites.

Figs. 6 and 7 show that these materials are active catalysts for the Henry reaction. In addition, some clear trends can be discerned in the selectivity of the dendron composites (i.e. alcohol versus alkene formation). Fig. 8 shows the average selectivity for the samples as a function of dendron generation and amine (i.e. AMP versus PIP) identity. As can be seen in all cases, the selectivity to the nitroalcohol is very high (over 70%), and it can be observed that the nitroalcohol selectivity increases with increasing dendrimer generation and in going from primary amines to secondary amines. The error bars shown indicate one standard deviation from the average selectivity over the reaction run. That the selectivity to the alcohol is highest with the PIP samples and that it increases with increasing dendrimer generation are consistent with previous

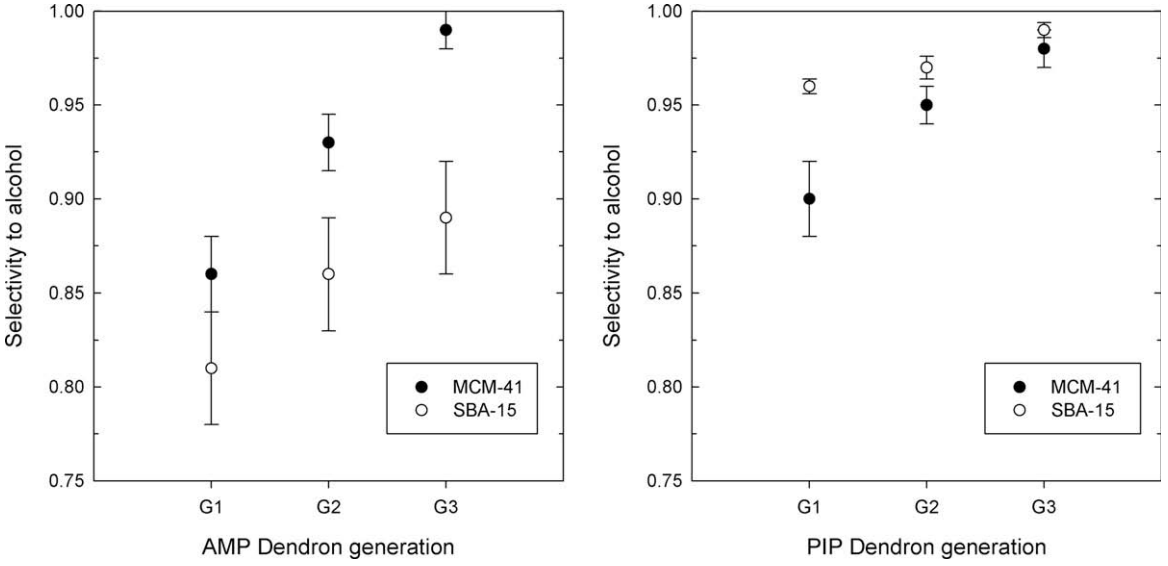

Fig. 8. Selectivity to the nitroalcohol product for the AMP (left) and PIP (right) dendrons.

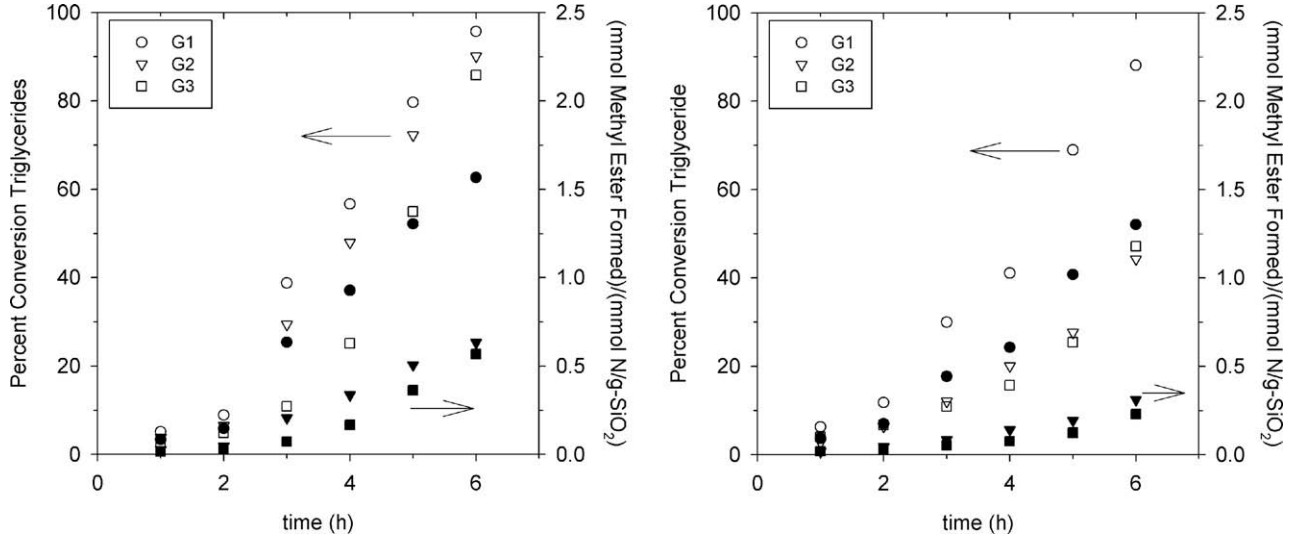

Fig. 9. Conversion of triglyceride (left axis) and mmol methyl ester formed per mmol nitrogen per gram of silica (right axis) versus time for AMP (left) and PIP (right) dendrons supported on MCM-41. Dendron generation denoted, solid symbols correspond to right axis, open symbols to left axis.

work by Katz as well as work from Asefa's laboratory [36,52,53]. Katz invokes a bifunctional surface to generate the alkene [36], and in the case of the G3 dendrons one might expect that many of the amines are far enough from the surface that amine–silanol cooperativity effects are not observed. It is also worth noting that the 'initial' selectivity to the alcohol (at 15 or 30 min into the reaction) is always higher than the average selectivity shown in Fig. 8. This would seem to indicate that it is possible for the alcohol to undergo subsequent dehydration to the olefin product. Plots of selectivity versus time for all samples can be found in the Supplementary material.

3.3. Transesterification reaction

Biodiesel, which is derived from triglycerides by transesterification with methanol, has attracted considerable attention during the past decade as a renewable, biodegradable, and nontoxic fuel [54–58]. Fig. 9 shows conversion of triglyceride to methyl ester over dendron-MCM-41 hybrids at 338 K. The conversion is highest over the G1 samples, again consistent with diffusion resistances. The primary amine-terminated dendrons are slightly more active than the secondary amine-terminated dendrons based on the results shown in Fig. 9. Fig. 10 shows the same chemistry performed over SBA-15 dendron hybrids. The results shown in Fig. 10 support the idea of diffusion resistances being present in the MCM-41 materials. The amount of methyl ester formed, particularly on a per mmol nitrogen basis, is significantly higher in the SBA-15 samples than in the MCM-41 samples. One can also see from the results shown in Fig. 10 that the primary amines are significantly more active than the secondary amines in forming methyl esters.

While the conversions observed over these materials are encouraging the most significant result is their stability. Fig. 11 shows the conversion of triglyceride after 6 h as a function of catalyst recycle number. As can be seen there are only very modest decreases of conversion with multiple recycles. This is in contrast to previous work from our laboratory where simple aminosilane groups attached to OMS were used as catalysts for this reaction [59]. Thus the materials formed possess reasonable activity and stability. This is attributed to the dendron structure inhibiting the solvent from cleaving the silane attachment to the surface.

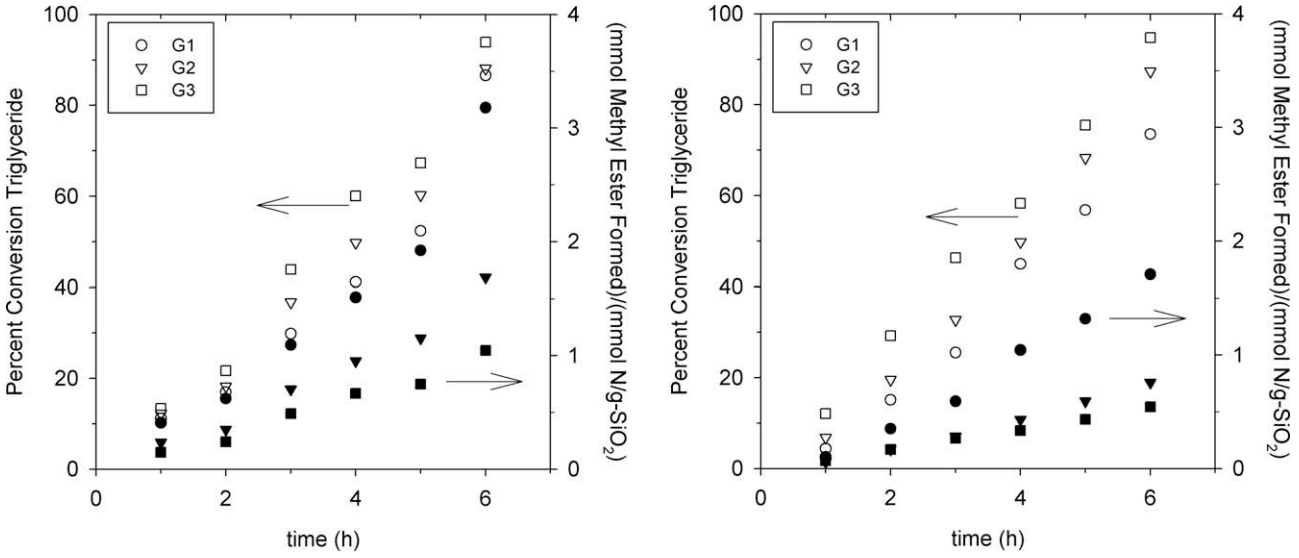

Fig. 10. Conversion of triglyceride (left axis) and mmol methyl ester formed per mmol nitrogen per gram of silica (right axis) versus time for AMP (left) and PIP (right) dendrons supported on SBA-15. Dendron generation denoted, solid symbols correspond to right axis, open symbols to left axis.

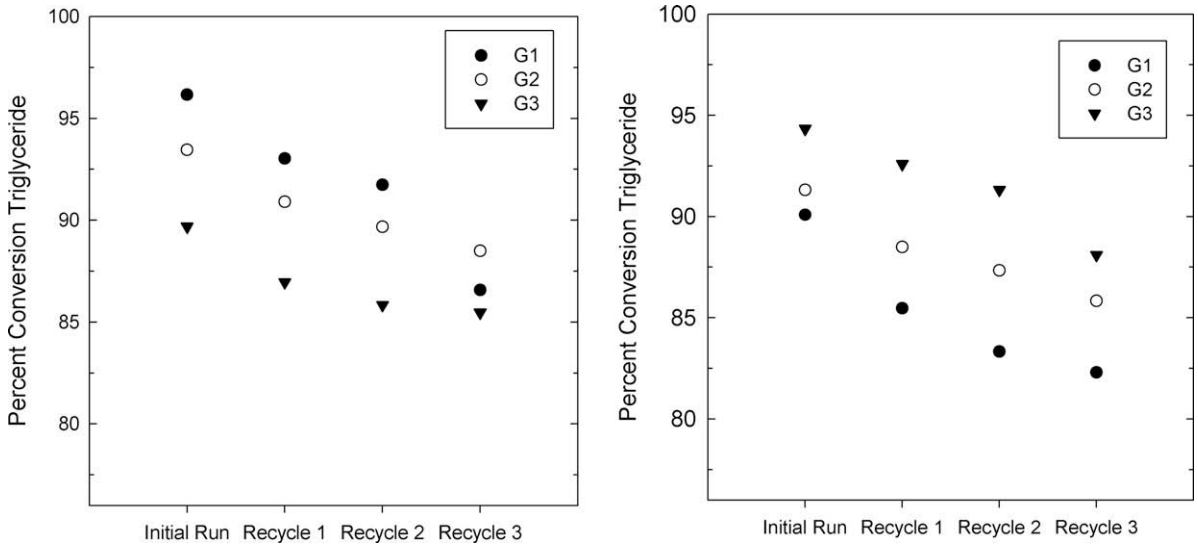

Fig. 11. Conversion after 6 h on stream versus recycle number for AMP MCM-41 (left) and AMP SBA-15 (right) dendron hybrids.

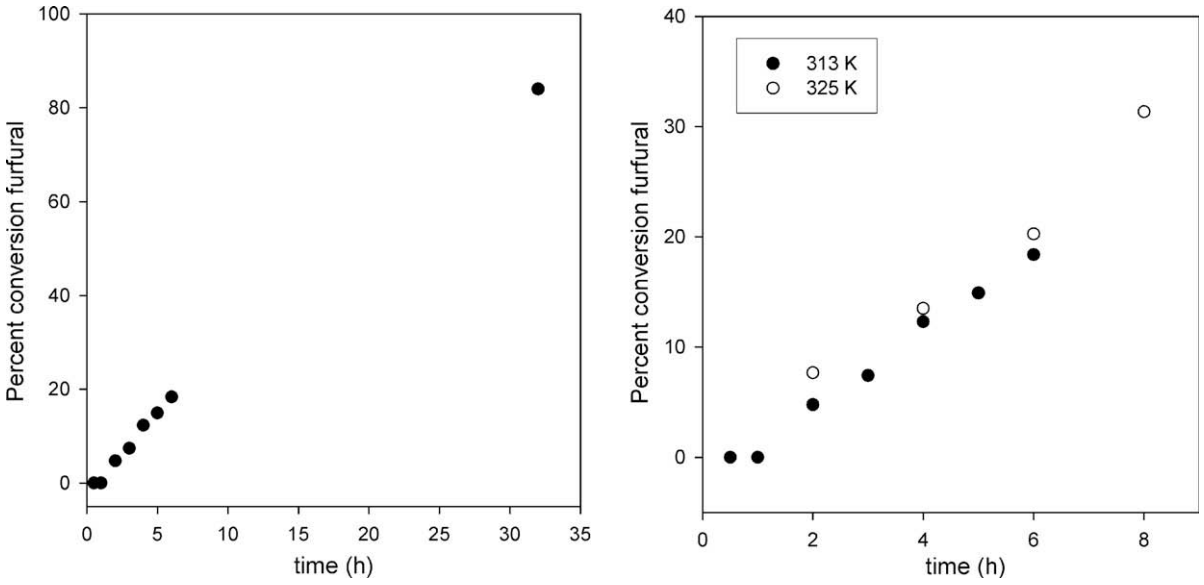

Fig. 12. Conversion of HMF over G1-PIP MCM-41.

Ongoing work is studying this in more detail as it relates to running reactions at higher temperatures.

3.4. Aldol coupling of HMF

The final reaction investigated was the condensation of 5-(hydroxymethyl)furfural (HMF) with acetone. This reaction represents a route to large alkanes in a biorefinery as HMF is formed via biomass hydrolysis and Aldol chemistry is often held up as a route to larger hydrocarbons from biomass precursors [60,61]. Fig. 12 shows the conversions versus time in the cross aldol condensation of HMF with acetone catalyzed by G1-PIP MCM-41. The conversion is 20% after 6 h of reaction and 80% after 32 h. The preliminary result shows that the dendron–OMS hybrids are active in this reaction; however, the reaction rate is lower than those in the previously discussed reactions. Ongoing work is investigating these reactions under higher temperature conditions and will be reported elsewhere.

4. Conclusions

The synthesis and catalytic testing of several dendron–OMS materials are reported. These materials show potential for a wide range of chemical reactions including Aldol chemistry and transesterification reactions. The results observed in the nitroaldol reaction are qualitatively consistent with the previous literature in terms of product selectivity, and the dendrons display good activity for this reaction. The dendron–OMS materials are not only active in the transesterification of triglycerides but also very stable. While possessing at best modest activity for the aldol reaction between HMF and acetone at 313 K, the results indicate that the OMS–dendron materials have potential as solid base catalysts for a range of reactions. Ongoing work is exploring additional chemistries, studying the thermal/solvothermal stability of the composites more carefully, and exploring multifunctional dendrons.

Acknowledgments

The authors acknowledge the National Science Foundation (CTS-0624813) for financial support of this work. Partial financial support was also provided by the Robert A. Welch Foundation (A-1638), Sabic Americas, CONACyT (V.V.G.), and LG Chemical (S.Y.).

Appendix A. Supplementary material

Diffraction patterns, nitrogen adsorption isotherms and α_s-analysis of all samples, summary of TGA/EA calculations for all samples. This information can be downloaded free of charge from the internet. Supplementary data associated with this article can be found, in the online version, at doi:10.1016/j.jcat.2009.10.009.

References

[1] D.M. Ford, E.E. Simanek, D.F. Shantz, Nanotechnology 16 (7) (2005) S458–S475.
[2] F. Hoffmann, M. Cornelius, J. Morell, M. Froba, Angew. Chem., Int. Ed. 45 (20) (2006) 3216–3251.
[3] K. Moller, T. Bein, Chem. Mater. 10 (10) (1998) 2950–2963.
[4] A. Taguchi, F. Schüth, Micropor. Mesopor. Mater. 77 (2004) 1–45.
[5] U. Ciesla, F. Schüth, Micropor. Mesopor. Mater. 27 (1999) 131–149.
[6] A. Corma, Chem. Rev. 97 (1997) 2373–2419.
[7] M.E. Davis, Nature 417 (2002) 813–821.
[8] F. Schüth, W. Schmidt, Adv. Mater. 14 (2002) 629–638.
[9] M.H. Lim, C.F. Blanford, A. Stein, J. Am. Chem. Soc. 119 (1997) 4090–4091.
[10] M.H. Lim, A. Stein, Chem. Mater. 11 (1999) 3285–3295.
[11] S.L. Burkett, S.D. Sims, S. Mann, Chem. Commun. (1996) 1367–1368.
[12] D.J. Macquarrie, Chem. Commun. (16) (1996) 1961–1962.
[13] C. Li, Catal. Rev. 46 (2004) 419–492.
[14] J.D. Bass, S.L. Anderson, A. Katz, Angew. Chem., Int. Ed. 42 (42) (2003) 5219–5222.
[15] J.D. Bass, A. Katz, Chem. Mater. 15 (2003) 2757–2763.
[16] J.D. Bass, A. Katz, Chem. Mater. 18 (6) (2006) 1611–1620.
[17] H.-T. Chen, S. Huh, J.W. Wiench, M. Pruski, V.S.Y. Lin, J. Am. Chem. Soc. 127 (2005) 13305–13311.
[18] J.L. Defreese, A. Katz, Chem. Mater. 17 (2005).
[19] G. Demicheli, R. Maggi, A. Mazzacani, P. Righi, G. Sartori, F. Bigi, Tetrahedron Lett. 42 (2001) 2401–2403.
[20] S. Huh, H.-T. Chen, J.W. Wiench, M. Pruski, V.S.Y. Lin, J. Am. Chem. Soc. 126 (2004) 1010–1011.
[21] S. Huh, H.-T. Chen, J.W. Wiench, M. Pruski, V.S.Y. Lin, Angew. Chem., Int. Ed. 44 (2005) 1826–1830.
[22] Y. Kubota, K. Goto, S. Miyata, Y. Goto, Y. Fukushima, Y. Sugi, Chem. Lett. 32 (2003).
[23] D.J. Macquarrie, R. Maggi, A. Mazzacani, M.J. Sabater, G. Sartori, R. Sartori, Appl. Catal. A 246 (2003) 183–188.
[24] K. Shimizu, H. Suzuki, E. Hayashi, T. Kodama, Y. Tsuchiya, H. Hagiwara, Y. Kitayama, Chem. Commun. (10) (2002) 1068–1069.
[25] K.-I. Shimizu, E. Hayashi, T. Inokuchi, T. Kodama, H. Hagiwara, Y. Kitayama, Tetrahedron Lett. 43 (2002).
[26] H. Yoshitake, E. Koiso, T. Tatsumi, H. Horie, H. Yoshimura, Chem. Lett. 33 (2004) 872–873.

[27] A. Corma, S. Iborra, I. Rodriguez, M. Iglesias, F. Sánchez, Catal. Lett. 82 (2002) 237–242.
[28] D. Dhar, I. Beadham, S. Chandrasekaran, Proc. Indian Acad. Sci. (Chem. Sci.) 115 (2003) 365–372.
[29] V. Dufaud, M.E. Davis, J. Am. Chem. Soc. 125 (31) (2003) 9403–9413.
[30] R.K. Zeidan, V. Dufaud, M.E. Davis, J. Catal. 239 (2006) 299–306.
[31] E.L. Margelefsky, A. Bendjeriou, R.K. Zeidan, V. Dufaud, M.E. Davis, J. Am. Chem. Soc. 130 (2008) 13442–13449.
[32] E.L. Margelefsky, R.K. Zeidan, V. Dufaud, M.E. Davis, J. Am. Chem. Soc. 129 (2007) 13691–13697.
[33] J.C. Hicks, R. Dabestani, A.C.I. Buchanan, C.W. Jones, Chem. Mater. 18 (2006) 5022–5032.
[34] J.C. Hicks, C.W. Jones, Langmuir 21 (2006) 2676–2681.
[35] M.W. McKittrick, C.W. Jones, Chem. Mater. 15 (2003) 1132–1139.
[36] J.D. Bass, A. Solovyov, A.J. Pascall, A. Katz, J. Am. Chem. Soc. 128 (11) (2006) 3737–3747.
[37] J.M. Rosenholm, A. Penninkangas, M. Linden, Chem. Commun. (37) (2006) 3909–3911.
[38] J.M. Rosenholm, A. Duchanoy, M. Linden, Chem. Mater. 20 (3) (2008) 1126–1133.
[39] K.Q. Yu, C.W. Jones, J. Catal. 222 (2) (2004) 558–564.
[40] J.C. Hicks, J.H. Drese, D.J. Fauth, M.L. Gray, G.G. Qi, C.W. Jones, J. Am. Chem. Soc. 130 (2008) 2902–2903.
[41] E.J. Acosta, C.S. Carr, E.E. Simanek, D.F. Shantz, Adv. Mater. 16 (12) (2004) 985–989.
[42] S. Yoo, J.D. Lunn, S. Gonzalez, J.A. Ristich, E.E. Simanek, D.F. Shantz, Chem. Mater. 18 (2006) 2935–2942.
[43] S. Yoo, S. Yeu, R.L. Sherman, E.E. Simanek, D.F. Shantz, D.M. Ford, J. Membr. Sci. 334 (2009) 16–22.
[44] J.P.K. Reynhardt, Y. Yang, A. Sayari, H. Alper, Chem. Mater. 16 (2004) 4095–4102.
[45] J.P.K. Reynhardt, Y. Yang, A. Sayari, H. Alper, Adv. Funct. Mater. 15 (2005) 1641–1646.
[46] P.J. Branton, K.S.W. Sing, J.W. White, J. Chem. Soc., Faraday Trans. 93 (1997) 2337–2340.
[47] K.J. Edler, J.W. White, Chem. Mater. 9 (5) (1997) 1226–1233.
[48] D.Y. Zhao, Q.S. Huo, J.L. Feng, B.F. Chmelka, G.D. Stucky, J. Am. Chem. Soc. 120 (24) (1998) 6024–6036.
[49] M. Jaroniec, M. Kruk, J.P. Olivier, Langmuir 15 (16) (1999) 5410–5413.
[50] F. Rouquerol, J. Roquerol, K. Sing, Adsorption by Powders and Porous Solids, Academic, San Diego, 1999.
[51] M. Morgenstern, J. Cline, S. Meyer, S. Cataldo, Energy Fuel 20 (2006) 1350–1353.
[52] A. Anan, R. Vathyam, K.K. Sharma, T. Asefa, Catal. Lett. 126 (1–2) (2008) 142–148.
[53] K.K. Sharma, T. Asefa, Angew. Chem., Int. Ed. 46 (16) (2007) 2879–2882.
[54] A. Cauvel, G. Renard, D. Brunel, J. Org. Chem. 62 (3) (1997) 749–751.
[55] M. Di Serio, M. Ledda, M. Cozzolino, G. Minutillo, R. Tesser, E. Santacesaria, Ind. Eng. Chem. Res. 45 (9) (2006) 3009–3014.
[56] M. Di Serio, R. Tesser, L. Pengmei, E. Santacesaria, Energy Fuel 22 (2008) 207–217.
[57] S. Gryglewicz, Bioresour. Technol. 70 (1999) 249–253.
[58] F. Ma, M.A. Hanna, Bioresour. Technol. 70 (1999) 1–15.
[59] V. Varela Guerrero, D.F. Shantz, Ind. Eng. Chem. Res. (ASAP article).
[60] G.W. Huber, J.N. Chheda, C.J. Barrett, J.A. Dumesic, Science 308 (2005) 1446–1450.
[61] J.N. Chheda, G.W. Huber, J.A. Dumesic, Angew. Chem., Int. Ed. 46 (2007) 7164–7183.